Supporting Information

Regulating the trap distribution of $ZnGa_2O_4$:Cr^{3+} by Li^+/Ga^{3+} doping for upconversion-like trap energy transfer NIR persistent luminescence

Junqing Xiahou[1], Qi Zhu[1*], Fan Li[1], Minghui Jin[1], Lin Zhu[2], Sai Huang[1], Tao Zhang[3], Xudong Sun[4], and Ji-Guang Li[5*]

[1]*Key Laboratory for Anisotropy and Texture of Materials (Ministry of Education), School of Materials Science and Engineering, Northeastern University, Shenyang, Liaoning 110819, PR China*

[2]*College of Sciences, Northeastern University, Shenyang Liaoning 110819, PR China*

[3]*Shenyang National Laboratory for Materials Science, Northeastern University, 3-11 Wenhua Road, Shenyang, Liaoning 110819, PR China*

[4]*Foshan Graduate School of Northeastern University, Foshan, Guangdong 528311, PR China*

[5]*Research Center for Functional Materials, National Institute for Materials Science, Namiki 1-1, Tsukuba, Ibaraki 305-0044, Japan*

*E-mail: zhuq@smm.neu.edu.cn and LI.Jiguang@nims.go.jp

Experimental section

Materials and synthesis

The Cr^{3+}-doped $Zn_{1-x}(Li/Ga)_xGa_2O_4$ (x=0-1) phosphors with the specially designed chemical compositions were synthesized by solid-state reaction using 99.99% pure ZnO, Ga_2O_3, Cr_2O_3, and Li_2CO_3 as the starting materials, which were all purchased from Aladdin Chemical Reagent Co. Ltd (Shanghai, China), respectively. Firstly, according to the chemical formula of $Zn_{1-x}(Li/Ga)_xGa_2O_4:0.005Cr^{3+}$, stoichiometric amounts of ZnO, Ga_2O_3, Cr_2O_3, and Li_2CO_3 were thoroughly mixed by grinding with an agate mortar and pestle for 30 minutes. The samples were then pre-fired in oxygen at 900 °C for 4 h in alumina crucible. After cooling to room temperature and regrinding for 30 min, the powder was heated at 1000 °C for 4 h in oxygen to produce the final phosphors. The heating rate for the two rounds of heating is 5 °C min^{-1}.

Surface functionalization

An amount of 100 mg of LGC powder was dispersed into 40 mL of sodium hydroxide solution (5 mmol/L), followed by 1 h sonication treatment. After stirring at room temperature for 24 h, the large-sized particles were removed through centrifuging the resulting suspension at 1000 rpm for 10 min. Finally, the as-obtained LGC-OH particles were collected by centrifuging the supernatant at 10 000 rpm for 10 min, which were then washed three times by deionized water. A mixture containing 10 mg of LGC-OH particles and 4 mL of dimethylformamide (DMF) was prepared by 10 min sonication treatment, and then the suspension was vigorously stirred at room temperature for 1 day after adding 40 μL of 3-aminopropyltriethoxysilane (APTES). The resultant LGC-NH$_2$ particles were obtained by high-speed centrifugation at ten thousand rpm for 10 min. The unreacted APTES was removed by washing with DMF three times.

Characterization techniques

Phase identification was performed by X-ray diffractometry (XRD, Model SmartLab, Rigaku, Tokyo, Japan) operating at 40 kV/40mA using nickel-filtered Cu $K\alpha$ radiation and a scanning speed of 6.0° 2θ/min. Solid-state ^{7}Li NMR (nuclear

magnetic resonance) spectra were recorded on an Agilent 600 DD2 spectrometer (Agilent, USA, magnetic field strength 14.1 T), and the dipole decoupling magic-angle spinning (DD/MAS). The resonance frequency for ^{7}Li is 233.0 MHz at room temperature. The spectra recycle delay is 3 s with a scanning number of 1200, and the test time is 1h with LiCl aqueous solution of 1mol/L as a reference for ^{7}Li chemical shift at 0 ppm. Solid-state ^{71}Ga DD/MAS NMR spectra were recorded on a Burker AVWBIII600 using the dipole decoupling magic-angle spinning (DD/MAS) in a 3.2-mm probe at room temperature. The resonance frequency for ^{71}Ga is 183.0 MHz. The spectra were obtained at a spinning speed of 12 kHz, and a recycle delay of 1 s. The scanning number is 3600, the sampling time is 1h, and the reference of ^{71}Ga chemical shift at 0 ppm was $Ga(NO_3)_2$ of 1.1mol/L. The Raman scattering measurements were carried out using a Raman microscope (Model R-XploRA Plus, Horiba, Kyoto, Japan) with a 532 nm He-Ne laser as the excitation source. The laser power was 49.1 mW at the sample. The data for Rietveld refinement were collected in the step-scan mode over the 2θ range of 10-120°, using a step interval of 0.02° and a counting time of 1 s per step. Rietveld refinement of the XRD patterns was carried out using the TOPAS 4.2 software. The diffuse reflectance (DR) spectra were obtained with a UV-Vis-NIR spectrophotometer (UV-3600 Plus, Shimadzu, Kyoto) equipped over the range of 200-800 nm using $BaSO_4$ powder as a standard reference with a 150 mm diameter integrating sphere. The photoluminescence (slits: 2 nm, 2 nm) and dynamic PersL (slits: 20 nm, 20 nm) spectra of phosphors were taken by Model JY FL3-21 spectrophotometer (Horiba, Kyoto) using a 450 W xenon lamp for excitation, a scan speed of 500 nm min^{-1} and a slit-width of 2 nm for both excitation and emission. The NIR afterglow was taken picture by a P4-0118 night-vision device. Before thermoluminescence (TL) measurements, the samples were exposed under the 254-nm UV light (15W) and ~740 nm NIR LED lamp (25 W). The TL glow curves were recorded using an FJ427A1 thermoluminescent dosimeter (Beijing Nuclear Instrument Factory) at a heating rate of 1 K·s^{-1}. An In-Vivo Imaging System (Kodak FX Pro, USA) in a dark environment took the afterglow decay images and *in vivo* imaging.

Computational details

The calculations were carried out by using density functional theory (DFT), as implemented in the Vienna ab initio Simulation Package (VASP).[1, 2] The generalized gradient approximation (GGA) of Perdew, Burke, and Ernzerhof (PBE) were used to treat the exchange correlations.[3] The energy cut-off for the plane-wave basis set was kept at a fixed value of 520 eV. Structure optimization was accomplished until the force on each atom is less than 0.01 eV Å^{-1}.

Cytotoxicity assay

A CCK-8 (Cell Counting Kit-8) assay was employed to analyze the cytotoxicity of LGC-NH$_2$. Briefly, cells (RAW264, A549-1 and HEK293T) were seeded into 96-well plates and cultured in an incubator (Thermo, USA) at 37 °C for 24 h with 5% CO$_2$ in the environment. After removing the old medium, new medium (100 μL/well) with different concentrations of LGC-NH$_2$ (10, 50, 100, 250, 500, and 1000 μg/mL) was added into the culture plates. Six experimental groups and one blank control group were set up. Each group of three duplicate wells was cultured in the incubator for 24 h. Subsequently, 10 μL of CCK-8 (10% of the medium volume) was added to each well for another 0.5 h culture. Then, a microplate reader (Thermo, USA) was employed to measure the absorbance at 450 nm.

In vivo imaging

The *x*=1 sample was chosen here for tissue imaging and *in vivo* imaging. In order to obtain the nanoparticles-NH$_2$ probes, the *x*=1 sample nanoparticles collected by sieving were treated using a two-step functionalization processing, which was described in our previous work. After functionalization, the resulting nanoparticles-NH$_2$ probes have better glucose-solubility and biocompatibility. Therefore, a luminescence solution was easily obtained by dispersing the nanoparticles-NH$_2$ probes in glucose solution. Before the in *vivo* imaging experiment, the nanoparticles-NH$_2$ glucose solution (1 mg·mL^{-1}) was exposure to the 254-nm UV light for 10 minutes. After irradiation process, 500 μL of the irradiated aqueous solution was injected into a nude adult mouse by subcutaneous on the belly. A Kodak In-Vivo Imaging System FX Pro was employed to monitor the signals of NIR afterglow in

living mouse without an illumination source in the whole process. For the *in vivo* recharge imaging experiment, a ~740 nm NIR LED lamp (25 W) was used as the light source for *in situ* excitation for 20 min. The exposure time for taking picture was set as 45 s. The university animal care and use committee approved the animal experiments and studies.

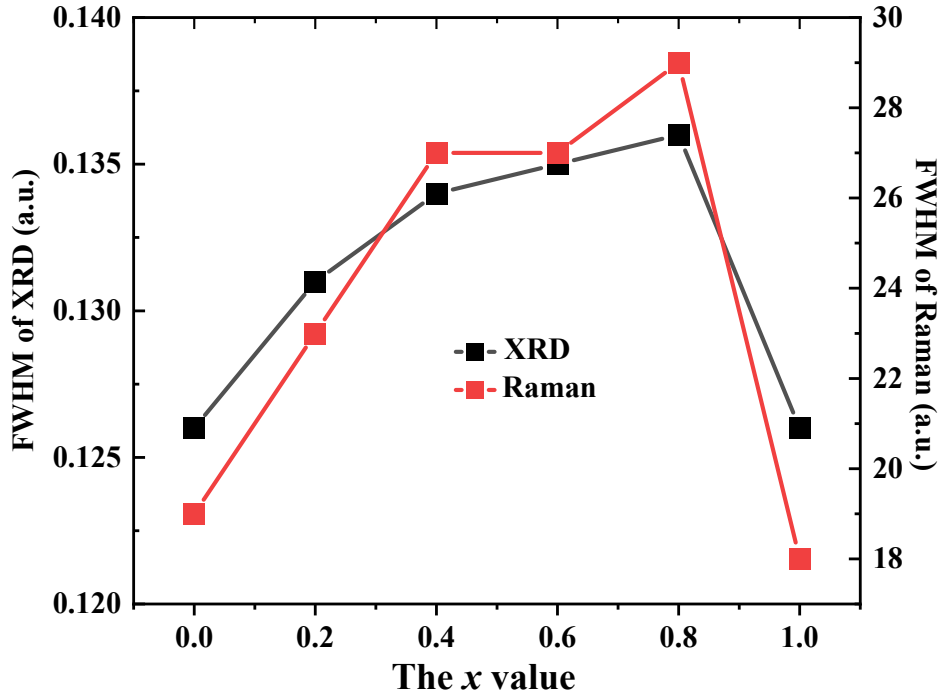**Table S1**. Table of lattice constant (*a/b/c*) of ZLGGC.

Sample	*x*=0	*x*=0.2	*x*=0.4	*x*=0.6	*x*=0.8	*x*=1
a/b/c	8.338	8.302	8.287	8.258	8.226	8.203
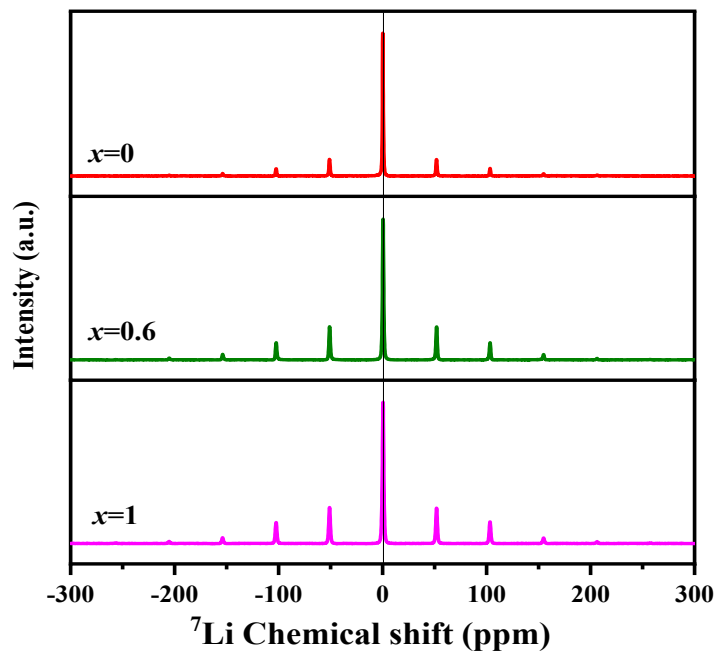
Figure S1. ^{7}Li MAS NMR spectra of ZLGGC.
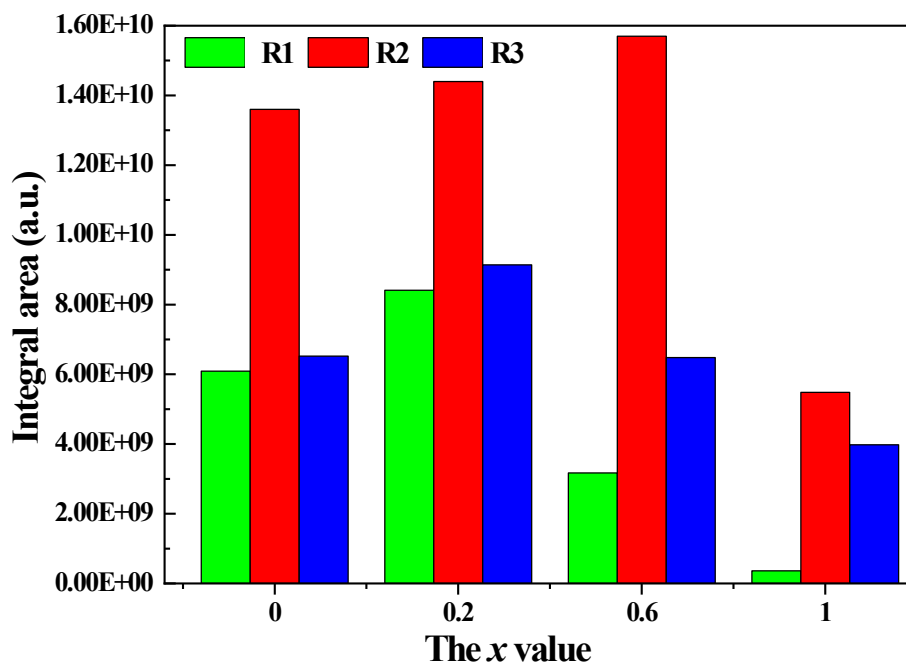
Figure S2. Integral areas of R1, R2, and R3.

Figure S3. FWHM of XRD patterns and Raman spectra.

Table S2. Structural parameters of ZLGGO obtained from the Rietveld refinement of X-ray diffraction data at room temperature.

The x value	$x=0$	$x=0.2$	$x=0.6$	$x=1$
Space group	Fd**Error!**m	Fd**Error!**m	Fd**Error!**m	$P4_332$
$a/b/c$ (Å)	8.338016(26)	8.30808(23)	8.27124(12)	8.20318(35)
V (Å^3)	579.680(20)	573.458(47)	565.864(24)	551.844(11)
2θ-interval (°)	10-120	10-120	10-120	10-120
Number of reflections	23	23	23	61
R_{wp} (%)	9.01	8.79	8.72	9.73
R_{ewp} (%)	6.15	6.14	6.27	8.18
R_p (%)	5.17	5.64	5.70	6.01
$\chi 2$	1.47	1.43	1.39	1.19
R_B	0.390	0.291	0.628	0.925

Table S3. Atomic positions of $ZnGa_2O_4$ (x=0) sample obtained from the room temperature Rietveld refinement of X-ray diffraction data.

Atom	Site	x	y	z	Occ.	B_{iso} (Å^2)
Zn1	8a	0.125	0.125	0.125	0.968	0.793(21)
Ga2	8a	0.125	0.125	0.125	0.032	0.793(21)
Ga1	16d	0.5	0.5	0.5	0.984	0.861(36)
Zn2	16d	0.5	0.5	0.5	0.016	0.861(36)
O1	32e	0.2621(13)	0.2621(13)	0.2621(13)	1	0.715(29)

Table S4. Atomic positions of $Zn_{0.8}Li_{0.1}Ga_{2.1}O_4$ (x=0.2) sample obtained from the room temperature Rietveld refinement of X-ray diffraction data.

Atom	Site	x	y	z	Occ.	B_{iso} (Å^2)
Zn1	8a	0.125	0.125	0.125	0.8	0.814(16)
Ga2	8a	0.125	0.125	0.125	1	0.814(16)
Li1	8a	0.125	0.125	0.125	0.1	0.814(16)
Ga1	16d	0.5	0.5	0.5	0.1	0.792(21)
O1	32e	0.2603(16)	0.2603(16)	0.2603(16)	1	0.902(22)

Table S5. Atomic positions of $Zn_{0.4}Li_{0.3}Ga_{2.3}O_4$ (x=0.6) sample obtained from the room temperature Rietveld refinement of X-ray diffraction data.

Atom	Site	x	y	z	Occ.	B_{iso} (Å^2)
Zn1	8a	0.125	0.125	0.125	0.4	0.756(36)
Ga2	8a	0.125	0.125	0.125	0.4	0.756(36)
Li1	8a	0.125	0.125	0.125	0.2	0.756(36)
Ga1	16d	0.5	0.5	0.5	0.95	0.669(29)
Li2	16d	0.5	0.5	0.5	0.05	0.669(29)
O1	32e	0.2556(16)	0.2556(16)	0.2556(16)	1	0.782(42)

Table S6. Atomic positions of $LiGa_5O_8$ (x=1) sample obtained from the room temperature Rietveld refinement of X-ray diffraction data.

Atom	Site	x	y	z	Occ.	B_{iso} (Å^2)
Li1	4b	0.625	0.625	0.625	1	0.547(36)
Ga1	12d	0.125	0.375	0.875	1	0.632(28)
Ga2	8c	0	0	0	1	0.726(31)
O1	8c	0.375	0.375	0.375	1	0.871(23)
O1	24e	0.125	0.125	0.125	1	0.743(40)
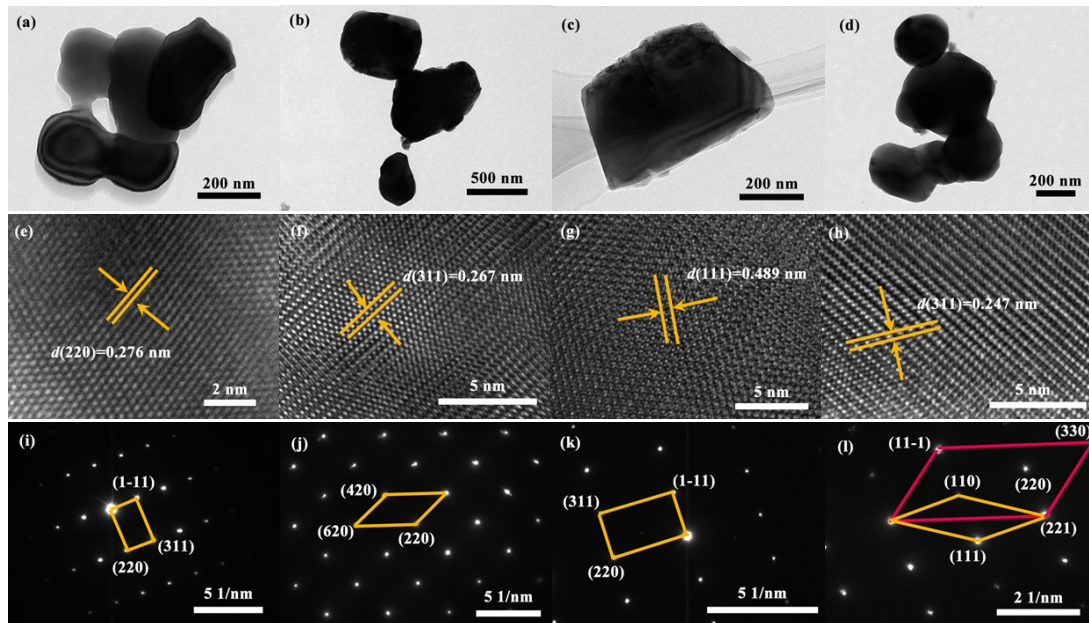
Figure S4. (a-d) TEM image, (e-h) HR-TEM lattice fringes, and (i-l) SAED patterns for ZLGGO samples. $x=0$: (a), (e) and (i); $x=0.2$: (b), (f) and (j); $x=0.6$: (c), (g) and (k); $x=1$: (d), (h) and (l).
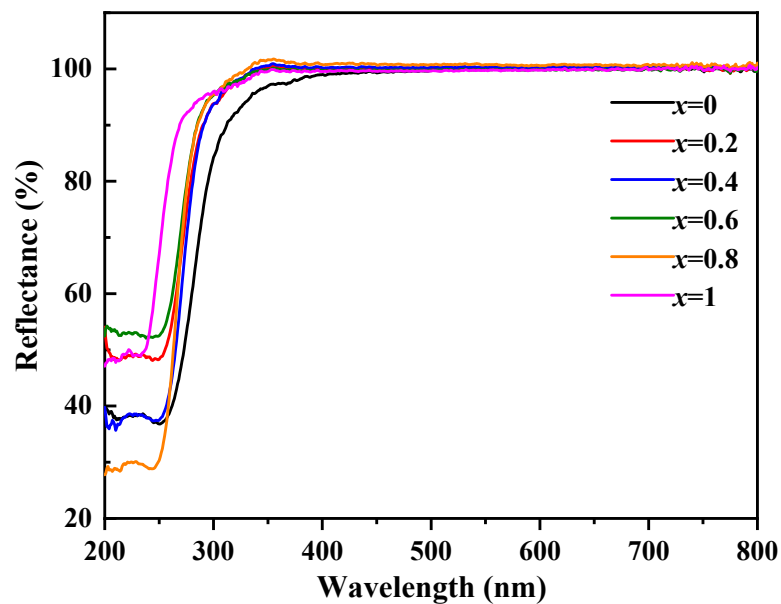
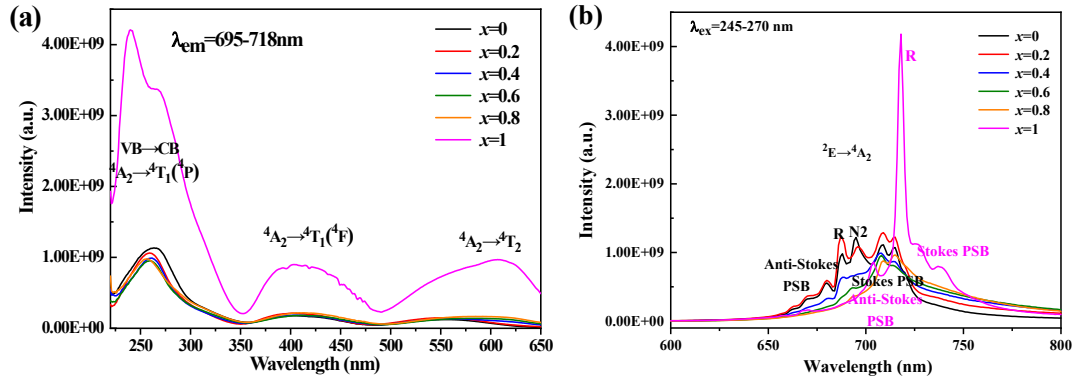**Figure S5.** The diffuse reflectance (R_{∞}) of ZLGGO.

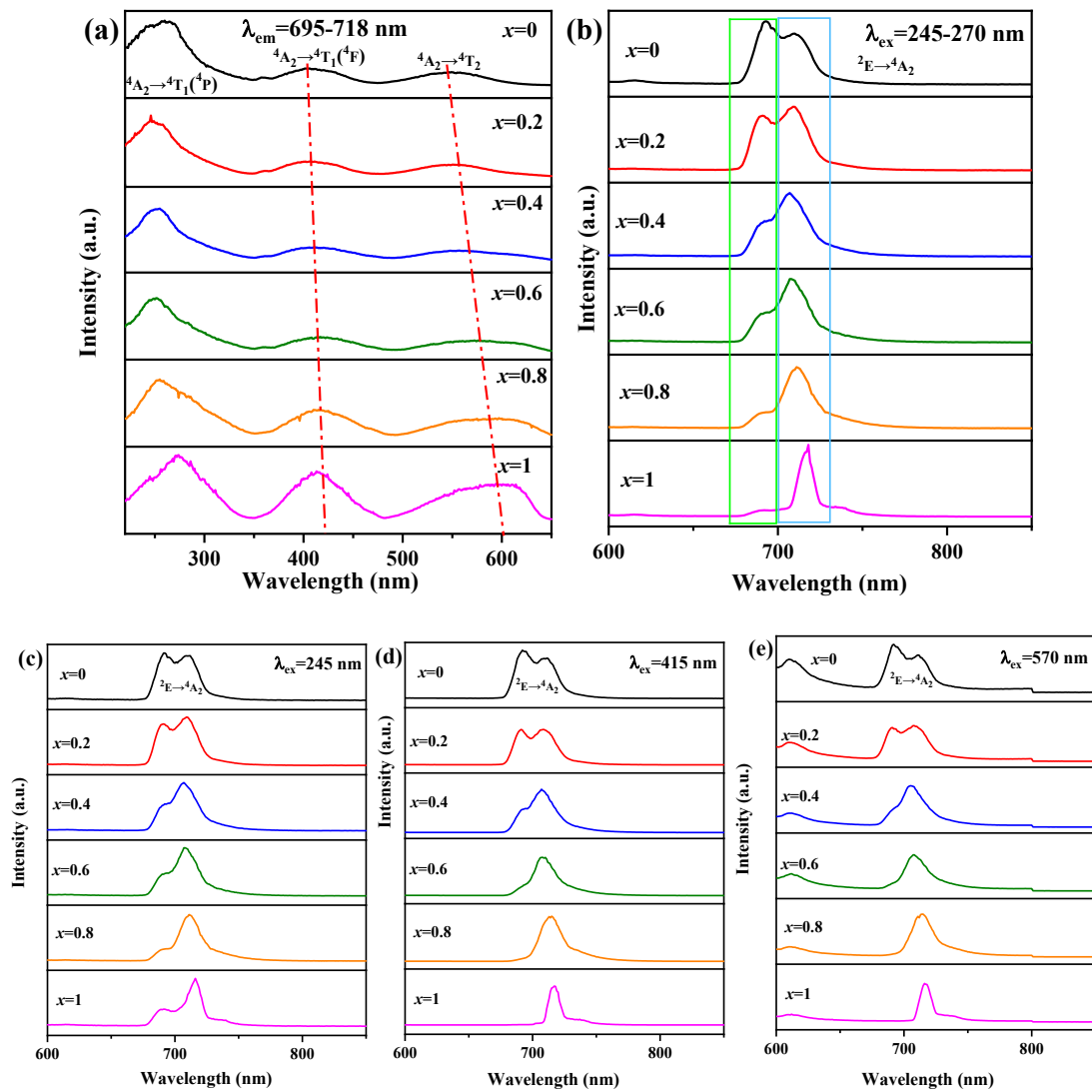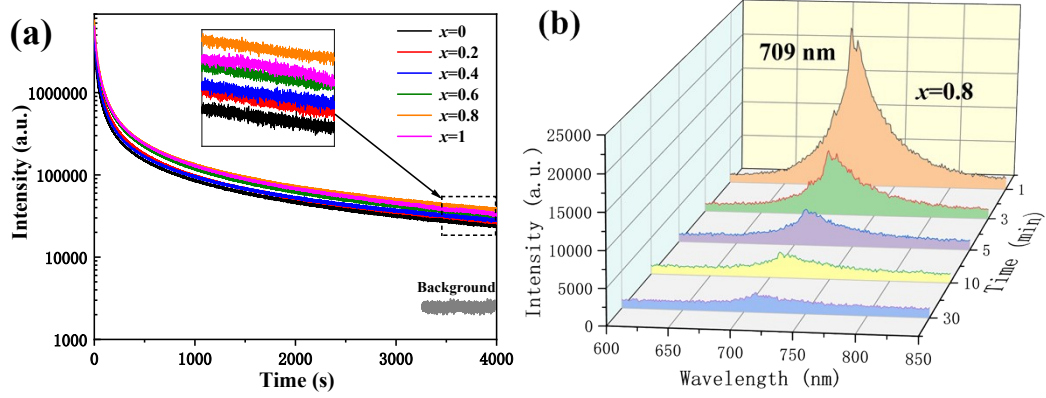**Figure S6.** (a) PLE and (b) PL spectra of ZLGGC at room temperature.

Figure S7. (a) PLE and (b-e) PL spectra of ZLGGC at 77K.

Figure S8. (a) Persistent luminescence decay curves of ZLGGC samples monitored at 695-718 nm after 254 nm UV light illumination for 10 min. (b) Persistent luminescence spectra of ZLGGC (*x*=0.8) measured at different times after pre-irradiation by 254 nm light illumination for 10 min.
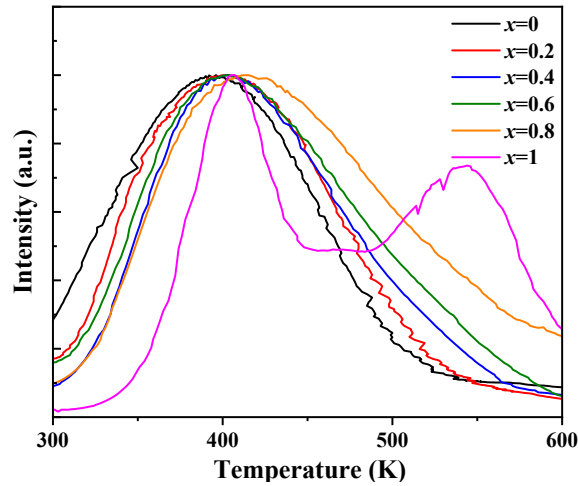
Figure S9. Normalized TL spectra of ZLGGC after 254 nm light illumination for 10 min.

Table S7. The parameters of the TL curves of ZLGGC samples.

Samples	T_m (K)	T_1 (K)	T_2 (K)	μ_g	I_m	E (eV)	n
x=0	396	325	464	0.486	10449	0.792	9.7510^6
x=0.2	398	334	475	0.563	11697	0.796	13.39×10^6
x=0.4	401	345	489	0.606	13041	0.802	15.78×10^6
x=0.6	402	342	495	0.608	13716	0.804	18.61×10^6
x=0.8	415	349	522	0.618	15091	0.83	23.73×10^6
x=1	405	375	445	0.572	13582	0.81	7.73×10^6

$$E = T_m/500 \qquad (1)$$

$$\text{And } n = \omega I_m/\{\beta \times [2.52 + 10.2 \times (\mu_g - 0.42)]\} \qquad (2)$$

where T_{m} is the temperature of peak maximum in TL curves (kelvin temperature). ω is the half-width defined as $\omega = T_2-T_1$, in which T_1, T_2 are the two half intensity temperatures and T_2 is the higher one. τ, δ are the low and high-temperature half-width defined as $\tau = T_m-T_1$, and $\delta=T_2-T_m$ respectively. $\mu_g = \delta/(\tau+\delta)$ reflects the symmetry properties, I_m is the intensity of the TL peak, and β represents the heating rate.
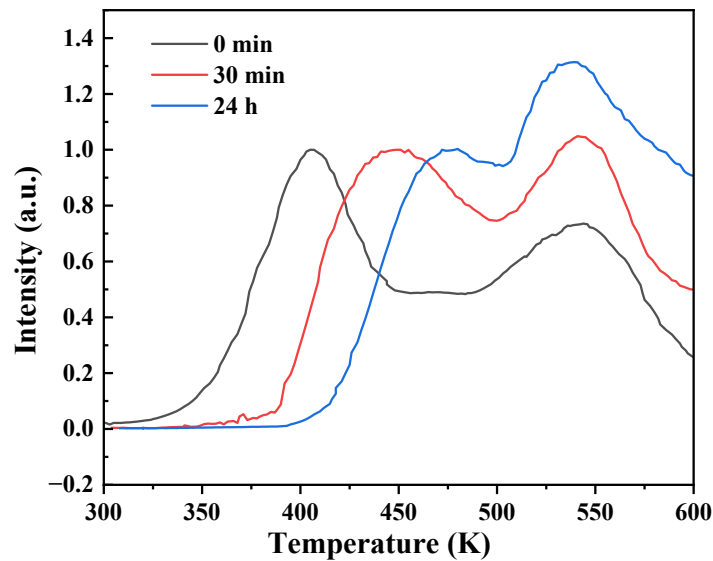

Figure S10. Normalized TL spectra of *x*=1 sample after ceasing the UV excitation (excitation wavelength: 254 nm; exposure time: 10 min; interval time: 0 min, 30 min, and 24 h.)
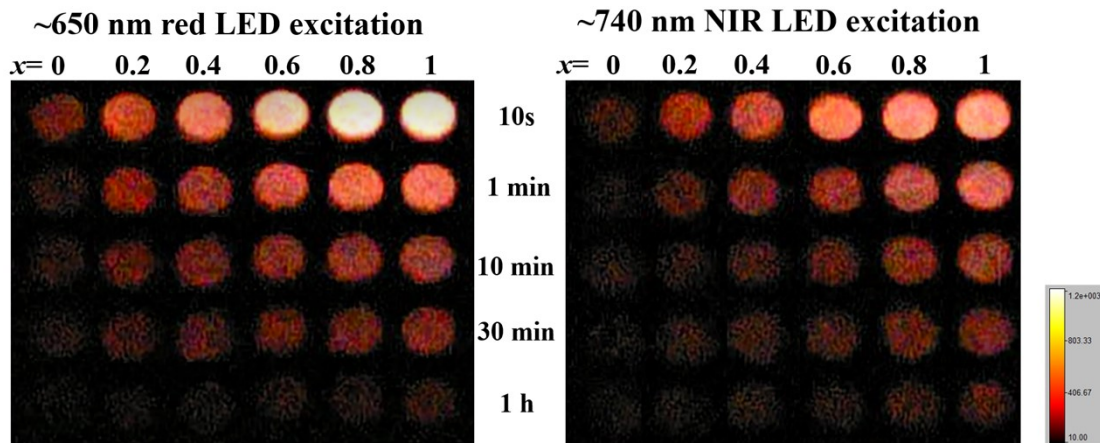
Figure S11. Time-dependent afterglows of ZLGGC phosphors with different ~650 nm red and ~740 nm NIR LED excitation.
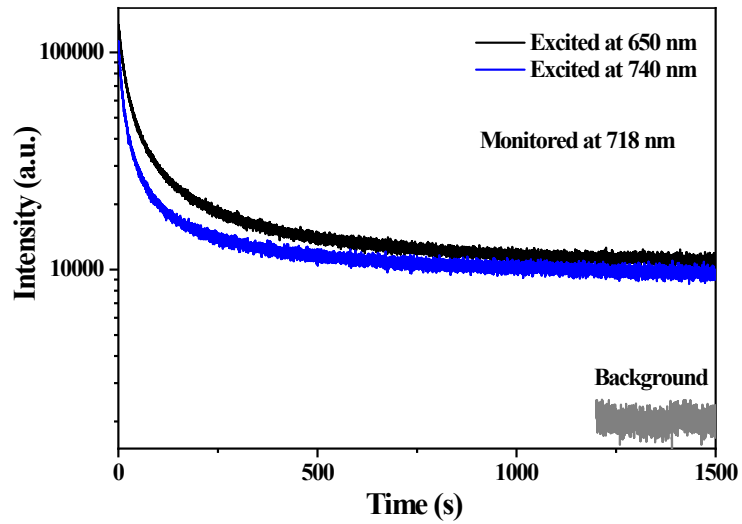
**Figure S12.** Afterglow decay curves of *x*=1 sample with different ~650 nm red and ~740 nm NIR LED excitation.
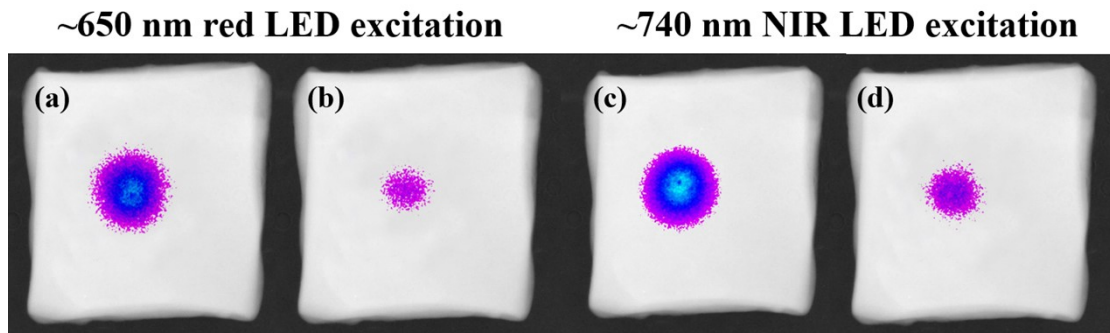
**Figure S13.** Afterglows of *x*=1 sample under the pork with different ~650 nm red and ~740 nm NIR LED excitation.

**Figure S14**. Real scenes of optical excitation of ZLGGC samples under the irradiation by ~740 nm NIR LED.
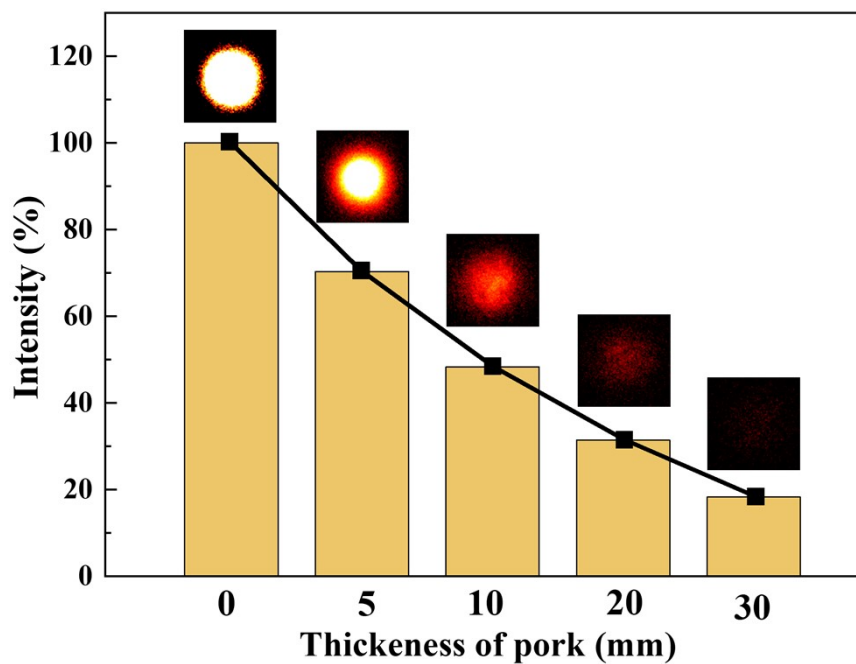
Figure S15. Rate variation of intensity reduction as a function of the pork thickness (0-30 mm) for *x*=1 sample.
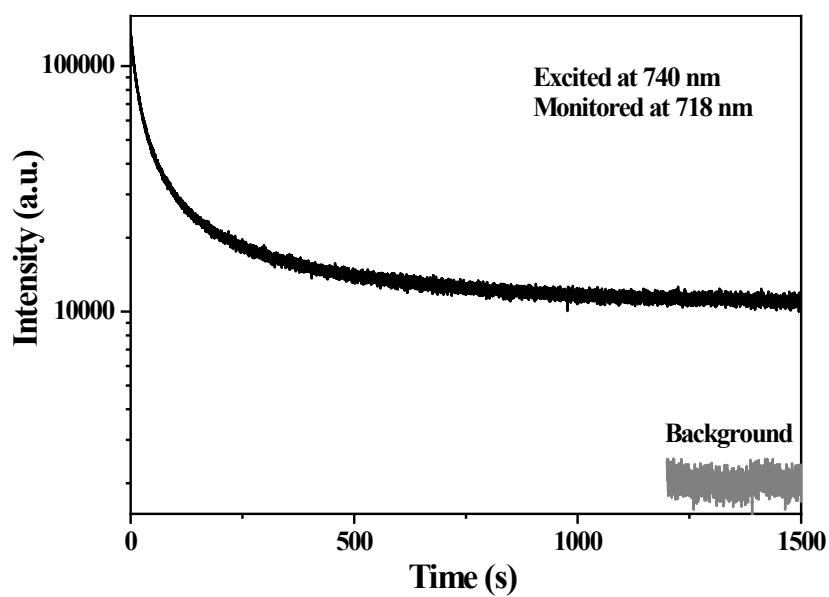
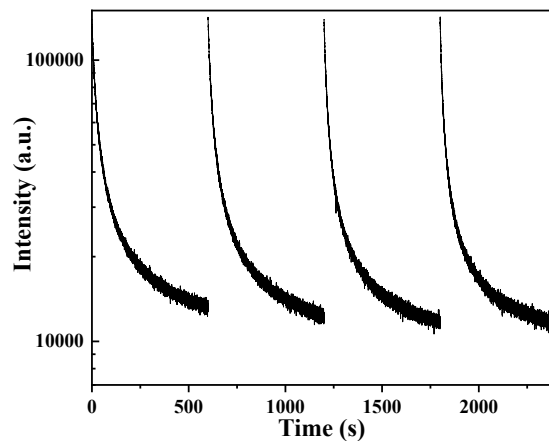**Figure S16.** Persistent luminescence decay curve of *x*=1 sample monitored at 718 nm after ~740 nm NIR LED illumination for 20 min.
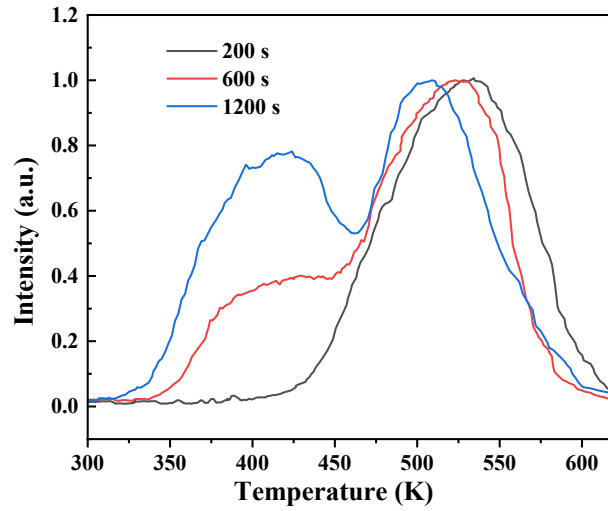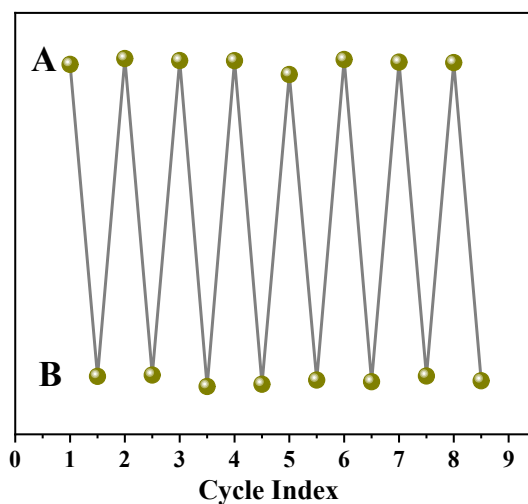
Figure S17. Normalized TL spectra of *x*=1 sample were measured using the ~740 nm NIR LED with different excitation times. (exposure time: 200, 600, and 1200 s)
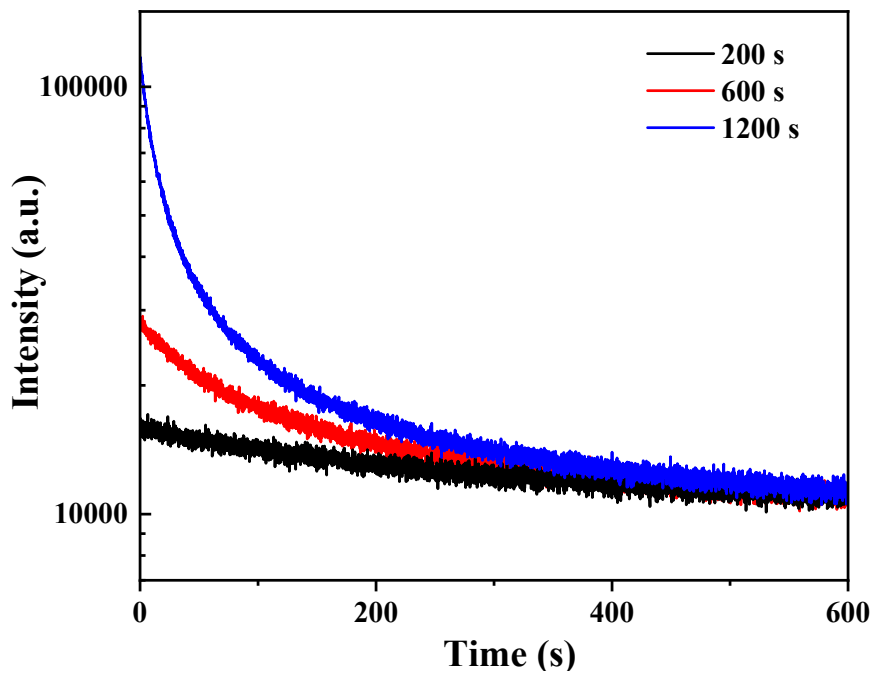
**Figure S18**. PersL decay curves of *x*=1 sample monitored at 718 nm emission after ~740 nm NIR LED excitation with different times.

Figure S19. Attenuating spectra of *x*=1 sample after four ~740 nm NIR LED irradiation.

Figure S20. Reproducibility of persistent luminescence under repeated excitation with NIR light from *x*=1 sample. A and B represent the PersL intensity after ceasing the NIR excitation at 1 s and that at 600 s, respectively.
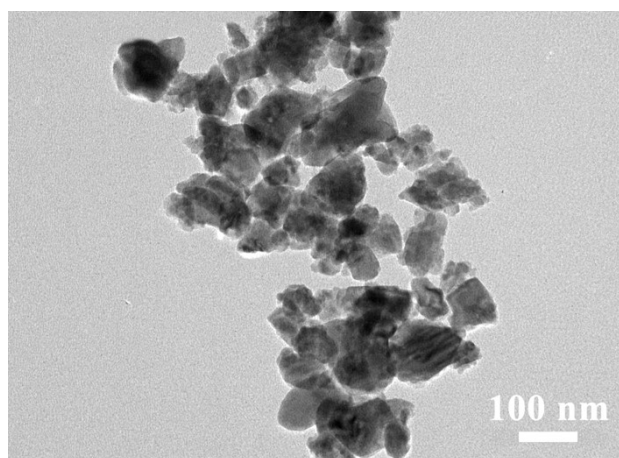
Figure S21. SEM image of *x*=1 sample nanoparticles collected by sieving.
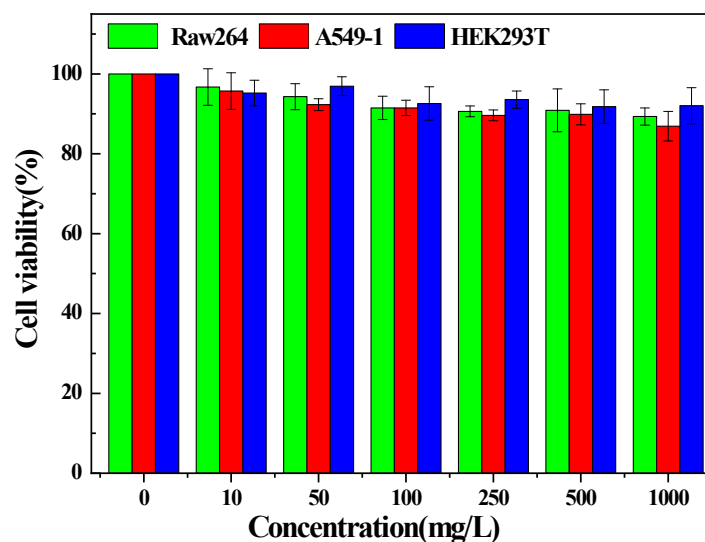
Figure S22. Cytotoxicity of LGC-NH$_2$ performed by the CCK-8 (Cell Counting Kit-8) assay with RAW264, A549-1, and HEK293T cells.

References

1.   P. E. Blochl, Projector augmented-wave method, *Physical review. B, Condensed matter*, 1994, **50**, 17953-17979.

2.   J. F. G. Kresse, Efficient iterative schemes for ab initio total-energy calculations using a plane-wave basis set, *Phys. Rev. B: Condens. Matter.*, 1996, **54**, 11169.

3.   J. P. Perdew, K. Burke and M. Ernzerhof, Generalized Gradient Approximation Made Simple, *Phys. Rev. Lett.*, 1996, **77**, 3865.